3D Reconstruction of CT images

A Term Paper as a Course requirement for

Master of Science (Mathematics)
With Specialization in Computer Science

Yogen Pradhan

21024

Supervised by - Dr.Srikanth Khanna

SRI SATHYA SAI INSTITUTE OF HIGHER LEARNING
(Deemed to be University)

Department of Mathematics and Computer Science
Prasanthi Nilayam Campus

November 2022

DECLARATION

The Term Paper titled **3D Reconstruction of CT Images** was carried out by me under the supervision of Dr.Srikanth Khanna, Department of Mathematics and Computer Science, Prashanti Nilayam Campus as a Course requirement for the Degree of Mathematics and Computer Science and has not formed the basis for the award of any degree, diploma or any other such title by this or any other University.

……..

Place : Prashanti Nilayam
Date : 26th November, 2022.

Yogen Pradhan
Reg no: 21024
II M. Sc. Mathematics
Prashanti Nilayam Campus

Abstract

As the medical field is growing rapidly, still there are questions on how to successful perform less risk prone surgery and increase success accuracy. The best solution so far is to make use of tomographic methods such as Computed Tomography(CT) with which the images are reconstructed of patient's internal organs. In situations,tomographic reconstruction can be derived simply mathematically which is changing sinogram to reconstructed image *i.e* finding inverse of Radon Transform. In this paper, we are analytically deriving the inverse using Filtered Backprojection . We are also optimizing the inverse using filters which helps it to perform better in real-world problems. Also we'll study what are methods like surface and volume rendering than analytical methods and look upon those methods help in reconstruction.

Keywords: CT, MRI, Sinogram, Backprojection, Segmentation, Contour , *Voxel*, Osteotomy , Fourier Transform, CCG

Dedicated to my beloved parents,

Acknowledgements

I would like to place my heartfelt gratitude to my parents who have encouraged me whenever I'm in need. Also I would like to thank my guide **Dr. Srikanth Khanna** who has given ample amount of time and helped me in clarifying all the doubts while doing this paper. I sincerely thank The Head of Department, **Dr. Raghunatha Sarma** for his constant encouragement and various inputs. I am thankful to the institute, Sri Sathya Sai Institute of Higher Learning and Department of Mathematics and Computer Science(DMACS) who provided me enough resources while completing this paper. I would like to thank my classmates for giving me constant support and assisting me in every way. Most importantly I place my heartfelt gratitude and love to our Dear Swami ,***Bhagawan Sri Sathya Sai Baba*** without whom this paper wouldn't be possible. I extend my thanks to all those whom I've inadvertently missed out to acknowledge.

Contents

List of Figures

Acronyms

CCG Custom Cutting Guide. 22, 25

CT Computed Tomography. 22, 26

DICOM Digital Imaging and Communications in Medicine. 16

FBP Filtered Backprojection. iv, 10

FDM Fused Deposition Model. 25

FFT Fast Fourier Transform. 27

FST Fourier Slice Theorem. iv, 9

HEA Hilgenreiner Epiphyseal Angle. 25

MPR Multiplanar Rendering. 17

MRI Magnetic Resonance Imaging. 26

1 Introduction

As there are many image modalities like CT, MRI which is basically looking at slices formed by these techniques but the 3D reconstruction of this slices remains the same. Sometimes while scanning for tumour, it happens that it is located somewhere behind bones thus there CT reconstruction helps by scanning it from various directions i.e taking many slices in tomographic reconstruction. For lower risk surgery and more accuracy we use computer based surgical planning which requires subtle amount of time in preoperatory planning and simulation which helps the doctors to correctly predict the outcome of the surgery.For this we need some mathematical background where this computer based surgical planning is useful. With enough preoperatory planning and all related reconstruction the risk of surgery is reduced and accuracy of surgery is increased highly for the doctors.

In this paper, the first part is entirely devoted to analytic method of tomography to reconstruct the image which basically have two approaches discrete and continuous. However this paper greatly deals about continuous approach and sought to derive mathematical model.

Second part deals on other methods and various state of art on this mathematical model which shows we can come up with optimization and new approaches other than analytical methods which enhances the image quality greatly and give more accuracy on reconstructed image and findings based on this mathematical model.

2 Mathematical Foundations

Analytically we can say that we are constructing the function f defined on the plane from the values of every straight line integral along f which becomes the fundamental problem of tomography. Let us now deduce how we can go through on getting this function f.

2.1 Approach

Let us make some assumptions to scale our problem and making it manageable:

1. The X-ray beam is single and infinitely thin and moves along a straight line.
2. Each beam travels through the same plane which is equivalent to single slice under examination.

For reconstruction we first put the slice into Cartesian coordinate and describe it as our object function f(x,y). The values of f for its corresponding slices are unknown to us but what is known to us is to visualize it as 2D image. What we know is the values of the function when a straight line l is passed through the slice thus we get f(l). Now we need to get f(x,y) from f(l). The obvious method is to backproject f(l) and get f(x,y) since *backprojection* is a method in which any function g(l) defined over set of lines in a plane can be converted into its corresponding function g(x,y) define over the plane. The known values f(l) is from sinogram of Radon Transform,but backprojection of f(l) doesnot lead us to f(x,y).So we have to find some other way to extract f(x,y) from f(l). We use *Fourier Transform* to change the domain of function and then we multiply the resultant function by a filter factor. After that we perform *Inverse Fourier Transform* to get the function defined over set of lines in frequency domain which is given by *Filtered Backprojection formula* and then we backproject the function to get our object function f(x,y).
Now we should know how this function f(l) is represented. We shall look upon *Beer's Law* to know what really is this function.

2.2 Beer's Law

When a ray of intensity I is passed it attenuates i.e its intensity decreases due to refraction or some other factors. If we considered that attenuated quantity as A the it is termed as attenuation coefficient. The relation is ;

$$I(x) = E.N(x)$$

where E is the energy of the ray anf N is number of photos it absorbs through x. For any time interval $\mathbf{\Delta}$x the proportion of photons absorbed is

$$p(x) = A(x).\Delta x$$

then multiplying this equation with intensity I(x) we get:

$$p(X)I(x) = A(x).I(x).\Delta x$$

Writing it in another form :

$$\Delta I = -A(x).I(x).\Delta x$$

then we get the expression of the beer law ;

$$dI/dx = -A(x).I(x) \tag{1}$$

Therefore the statement of *Beer's Law* states that the change of intensity over distance is proportional to both attentuation and intensity.[1]

For any time interval $\mathbf{x_0}$ with intensity $\mathbf{I_0}$ and $\mathbf{x_1}$ with intensity $\mathbf{I_1}$,solving equation (2.1) we get :

$$\int_{x_0}^{x_1} A(x)\,dx = ln(I_0/I_1) \tag{2}$$

In this equation (2.2) , we can tell that f(l) can be represented as line integral through a straight line l.[5]

[1] named after German scientist August Beer

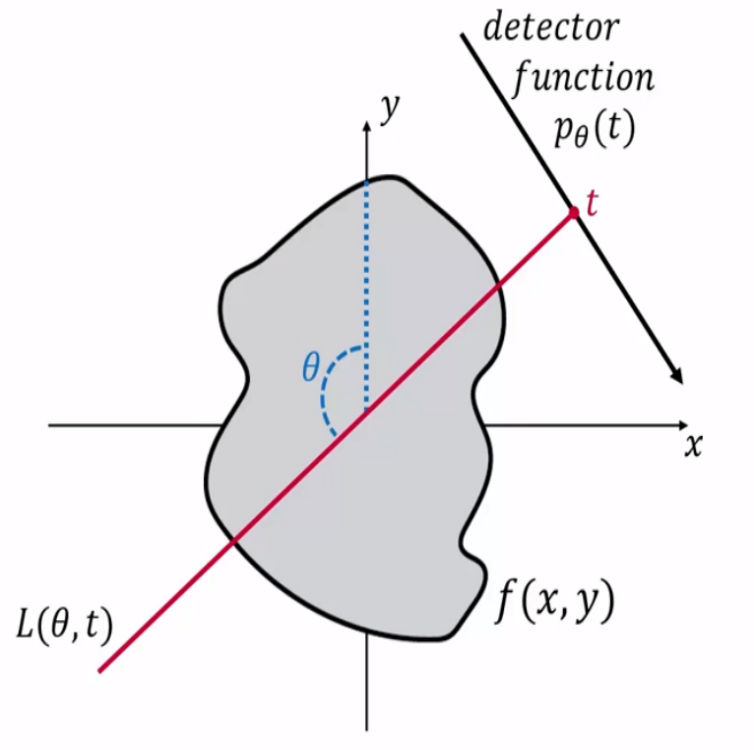

Figure 1: Illustration of Radon Transform

2.3 Radon Transform

Radon transform simply converts f(x,y) to f(l). Consider a object function f(x,y) and the detector function $\mathbf{P}_\theta(\mathbf{t})$, then the straight line passing through the object is $\mathbf{L}(\theta, \mathbf{t})$ with angle θ with the y axis then the transform of this projection is given by [12]:

$$P_\theta(t) = \int_{L(\theta,t)} f(x,y)\, ds$$

If we rotate the detector function 360° i.e we take more projection, then we get the corresponding Radon Transform:

$$Rf(x,t) = \int_{L(\theta,t)} f(x,y)\, ds \tag{3}$$

When the radon tranform is displayed as graph it is called sinogram.

Consider a straight line

$$y = ax + b$$

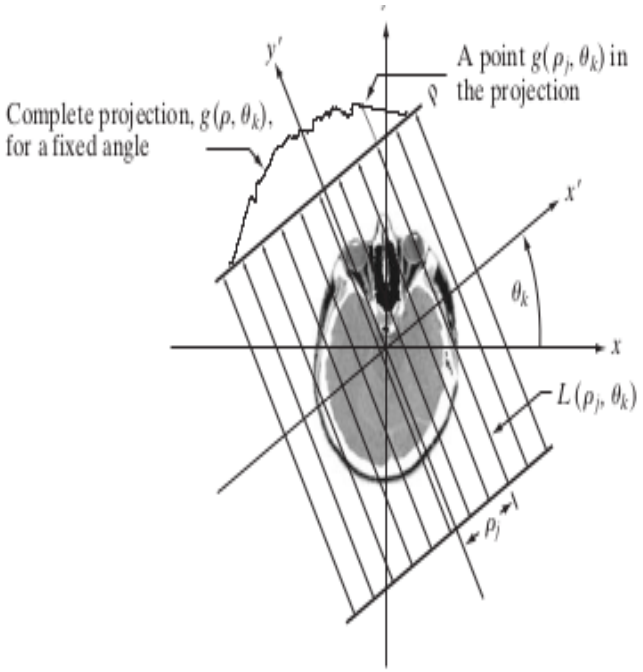

Figure 2: Radon Transform

or in normal representation

$$xcos\theta + ysin\theta = \rho$$

The ray sum is the line integral :

$$g(\rho_j, \theta_k) = \int_{-\infty}^{\infty} \int_{-\infty}^{\infty} f(x, y)\delta(xcos\theta_k + ysin\theta_k - \rho_j)\, dx\, dy \tag{4}$$

If we consider all the values of ρ and θ we get :

$$g(\rho, \theta) = \int_{-\infty}^{\infty} \int_{-\infty}^{\infty} f(x, y)\delta(xcos\theta + ysin\theta - \rho)\, dx\, dy \tag{5}$$

If we apply Radon transform on dirac delta function i.e when a point on Cartesian coordinate we get a sine wave of that point. So the projection of object function is sum of sine waves.

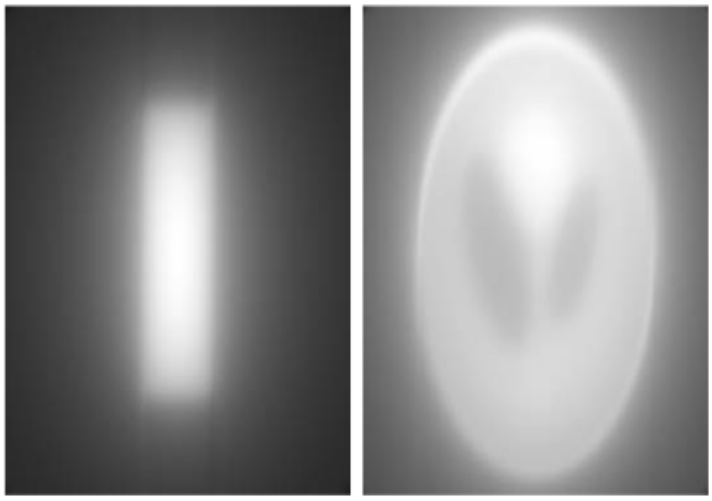

Figure 3: Backprojection of the sinograms of Rectangular and Shepp-Logan Phantom

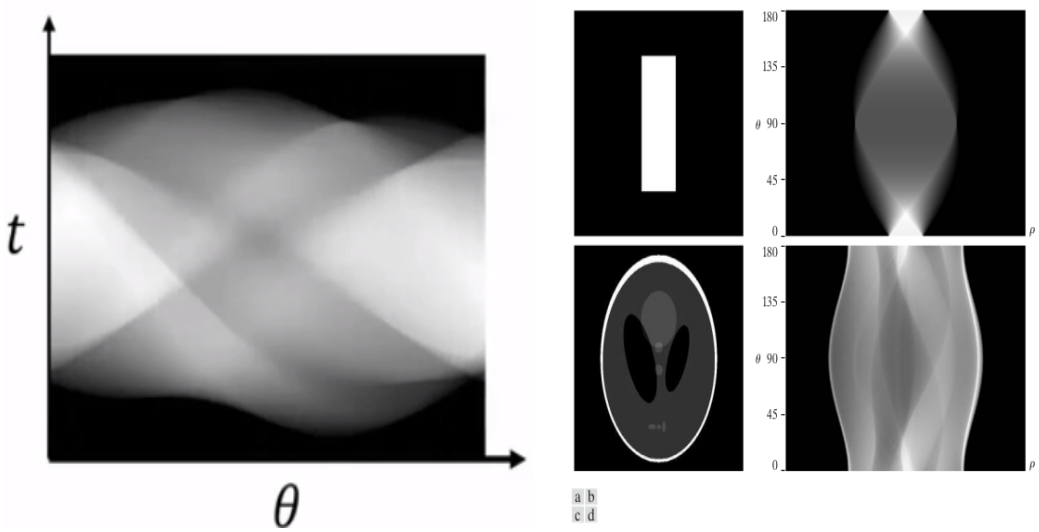

We take the sinogram of a rectangular object and *Shepp-Logan phantom*[4]

2.4 Backprojection

We can convert the function g(l) into f(x,y) using backprojection itself but the result we get is very bad as it distorts the original function. Since the backprojection is changing the domain of function from the set of all lines in the plane to the set of all coordinates in the plane. So we need to find some other techniques to filter the image as we see backprojection is not inverse of Radon Transform.

2.5 Fourier Transform

As backprojection gives blurry image that doesnot mean it is useless but with some filtering we can make use of it.o we need a function which is easily filterable and this is done using Fourier Transform. *Fourier Transform* basically deal with spatial domain and frequency domain. As the Fourier series and Fourier transform is applied on signals, it is to the fact the Fourier series is on periodic signals whereas Fourier transform is on non-periodic signals and since most images are non periodic we use the Fourier transform to convert the spatial domain into frequency domain.

Frequency Domain: The set where the frequencies of image can be represented.

Spatial Domain: Representation of image as function of points i.e all the points that a image can occupy.

Any periodic function can be expressed as weighted sum of sines and cosines(Fourier Series). Expressing the function as integral of sines and cosines multiplied by weighted function is Fourier Transform. The *one dimensional Fourier Transform* is given by:

$$f(\omega) = \int_{-\infty}^{\infty} f(x) e^{-i\omega x}\, dx \tag{6}$$

and its inverse is given by :

$$f(x) = 1/2\pi \int_{-\infty}^{\infty} g(\omega) e^{i\omega x}\, d\omega$$

The *two dimensional Fourier Transform* is given by:

$$F(\mu, v) = \int_{-\infty}^{\infty} \int_{-\infty}^{\infty} f(t, z) e^{-j2\pi(\mu t + vz)}\, dt\, dz \tag{7}$$

here μ and v are frequency variables and f(t,z) is continuous function. The inverse of 2D Fourier Transform is :

$$F(t, z) = 1/4\pi^2 \int_{-\infty}^{\infty} \int_{-\infty}^{\infty} f(\mu, v) e^{j2\pi(\mu t + vz)}\, d\mu\, dv$$

Lets us now see the relationship between Radon Transform and Fourier Transform in the next section .

2.6 Fourier Slice Theorem

The statement goes like this :

The Fourier Transform of a parallel projection of an object f(x,y) obtained at angle θ equals a line in a 2D Fourier transform of f(x,y) taken at the same angle.[5]

Here we form a relation between 1-D Fourier transform of a projection and 2-D Fourier transform of the region from which the projection was obtained. Denote f(x,y) as the object being reconstructed and p(t,θ) as parallel projection of f taken at angle θ,

t - represents the distance of the projection ray of the center of rotating.

Lets us prove the theorem now:

We know the 2D Fourier transform of a continuous function f(t,z) is :

$$F(\mu, v) = \int_{-\infty}^{\infty} \int_{-\infty}^{\infty} f(t, z) e^{-j2\pi(\mu t + vz)} \, dt \, dz$$

here μ and v are frequency variables.

Consider the 1D Fourier Transform of detector function wrt ρ :

$$P_\theta(\omega) = \int_{-\infty}^{\infty} p_\theta(t) e^{-i2\pi t} \, dt$$

The detector function $\mathbf{p}_\theta(\mathbf{t})$ is represented in its radon transform form i.e

$$p_\theta(t) = Rf(\theta, t) = \int_{L(\theta,t)} f(x, y) \, ds$$

So changing the notation we get

$$G(\omega, \theta) = \int_{-\infty}^{\infty} g(p, \theta) e^{-j2\pi\omega\rho} \, d\rho$$

Putting the value of equation (2.5) in the equation we get :

$$G(\omega, \theta) = \int_{-\infty}^{\infty} \int_{-\infty}^{\infty} f(x, y) [\int_{-\infty}^{\infty} \delta(xcos\theta + ysin\theta - \rho) e^{-j2\pi\omega\rho} \, d\rho] \, dx \, dy$$

$$= \int_{-\infty}^{\infty} \int_{-\infty}^{\infty} f(x, y) e^{-j2\pi\omega(xcos\theta + ysine\theta)} \, dx \, dy$$

This equation very much resembles to 2D Fourier transform of object function and we get

$$G(\rho, \theta) = F(\omega cos\theta, \omega sin\theta) \tag{8}$$

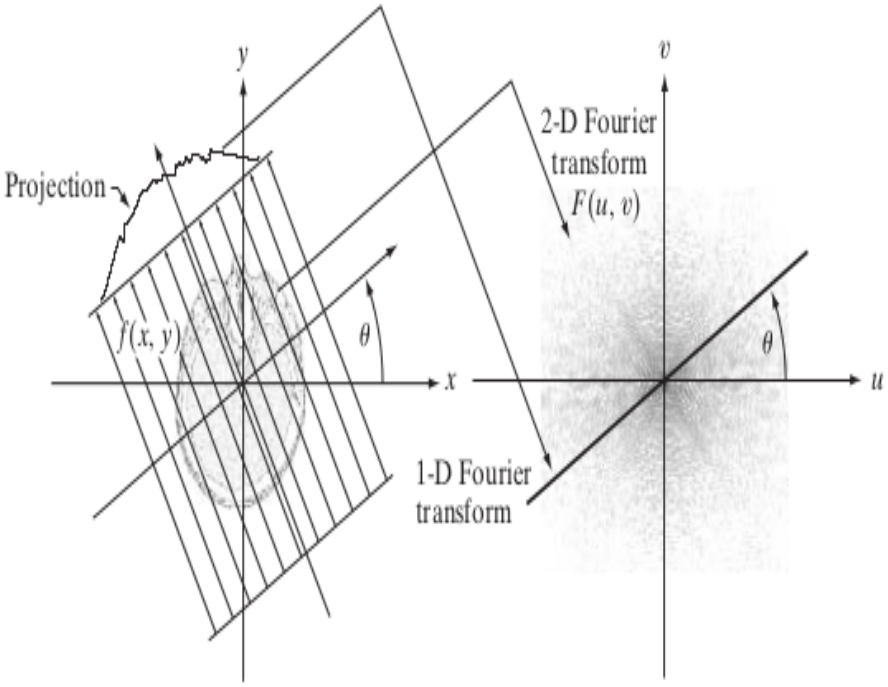

Figure 4: FST Illustration

$$G(\rho, \theta) = F(\omega cos\theta, \omega sin\theta)$$

2.6.1 Problems in FST

Since the image here is also blurry for the reconstructed object function . Also the sampling pattern we get is circular but what is needed in inverse Fourier transform is square type i.e Cartesian. So Fourier domain needs to be interpolated into Cartesian coordinates which is not at all easy as there can be lot of error as the interpolation is done on Fourier domain rather than real domain thus affecting the entire image with small error. Does that mean Fourier Slice theorem is useless ?? Not really , because this theorem serves as the basis to another reconstruction technique called Filtered Backprojection where the image we get is filtered as the inverse Fourier transform of FST is replaced by some other operator .[12]

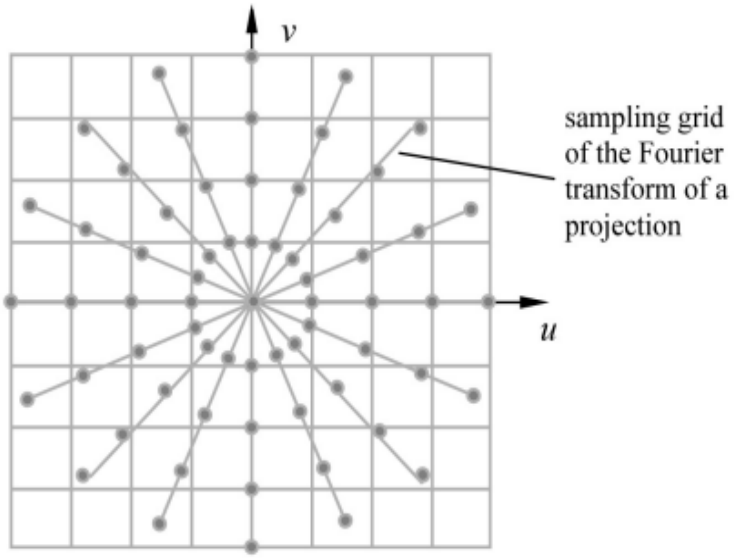

Figure 5: Fourier Sampling

2.7 Filtered Backprojection

There are two types of FBP depending on beams . We'll study each as follows :

2.7.1 Parallel Beam FBP

The image function f(x,y) from 2D inverse Fourier transform is :

$$f(x,y) = \int_{-\infty}^{\infty}\int_{-\infty}^{\infty} F(u,v)e^{j2\pi(ux+vy)}\,du\,dv$$

Transforming the Cartesian coordinate (u,v) to polar coordinate (ω,θ) by :

$$u = \omega cos\theta, v = \omega sin\theta \tag{9}$$

and

$$du\,dv = \omega\,d\omega\,d\theta$$

We get the following equation :

$$f(x,y) = \int_0^{2\pi} d\theta \int_0^{\infty} F(\omega cos\theta, \omega sin\theta)e^{j2\pi(xcos\theta+ysin\theta)}\omega\,d\omega \tag{10}$$

Using Fourier Slice Theorem by replacing F(ωcosθ,ωsinθ) with P(ω,θ) we get :

$$f(x,y) = \int_0^{2\pi} d\theta \int_0^{\infty} P(\omega,\theta) e^{j2\pi\omega(xcos\theta+ysin\theta)} \omega \, d\omega \tag{11}$$

$$= \int_0^{\pi} d\theta \int_0^{\infty} P(\omega,\theta) e^{j2\pi\omega(xcos\theta+ysin\theta)} \omega \, d\omega + \int_0^{\pi} d\theta \int_0^{\infty} P(\omega,\theta+\pi) e^{-j2\pi\omega(xcos\theta+ysin\theta)} \omega \, d\omega$$

In parallel sampling geometry ,

$$p(t,\theta+\pi) = p(-t,\theta)$$

also

$$P(\omega,\theta+\pi) = P(-\omega,\theta)$$

Substituting we get :

$$f(x,y)) = \int_0^{\pi} d\theta \int_{-\infty}^{\infty} P(\omega,\theta)|\omega| e^{j2\pi\omega(xcos\theta+ysin\theta)} \, d\omega \tag{12}$$

Expressing the equation in rotated coordinate system (s, t) we arrive at :

$$f(x,y) = \int_0^{\pi} d\theta \int_{-\infty}^{\infty} P(\omega,\theta)|\omega| e^{j2\pi\omega t} \, d\omega \tag{13}$$

where P(ω,θ) is the Fourier transform of projection at angle θ and inside integral is the inverse Fourier transform of P(ω,θ)| ω |. In spatial domain, it represents a projection filtered by a function whose frequency domain response is | ω | and is called "filtered projection".

2.7.2 Fan Beam FBP

Define two parameters α and β where γ is the angle formed by the ray with the iso-ray and β is the angle of the iso-ray formed with the y axis.

α - detector angle and specifies the location of a ray within the fan.

β - Projection angle and indicates which projection view is used.

The parameters of line $L(\rho,\theta)$ are related as :

$$\theta = \beta + \alpha, \quad t = Dsin\alpha$$

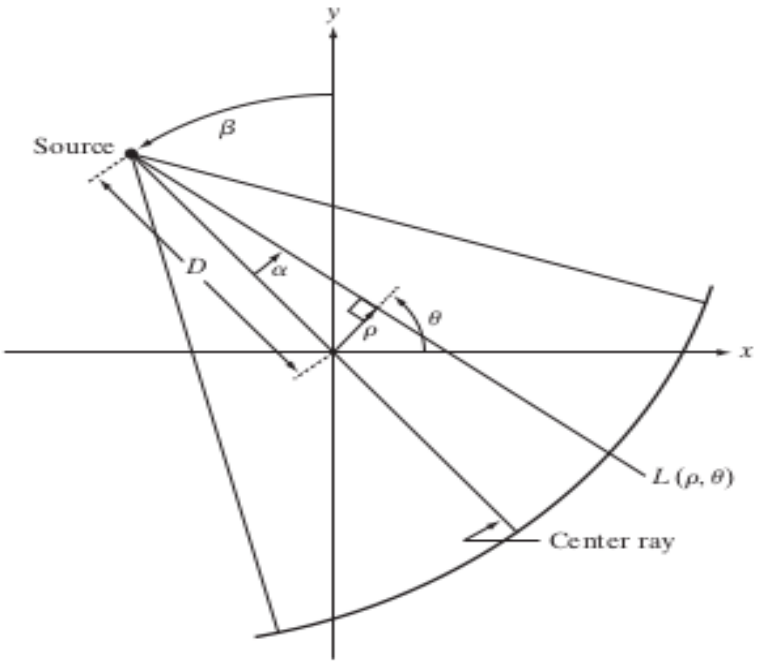

Figure 6: Feam Beam FST Illustration

where D is the distance between source and iso-center.

Modifying the above equation over 2π :

$$f(x,y) = 1/2 \int_0^{2\pi} \int_{-T}^{T} g(\rho,\theta) s(xcos\theta + ysin\theta - \rho)\, d\rho\, d\theta$$

In polar coordinates the equation becomes :

$$f(r,\phi) = 1/2 \int_0^{2\pi} \int_{-T}^{T} g(\rho,\theta) s(rcos(\theta - \phi) - \rho)\, d\rho\, d\theta$$

Writing the equation in terms of(α,β) and

$$d\rho\, d\theta = Dcos\alpha\, d\alpha\, d\beta$$

$$f(r,\phi) = 1/2 \int_{-\alpha}^{2\pi-\alpha} \int_{-\mathbf{sin^{-1}(-T/D)}}^{\mathbf{sin^{-1}(-T/D)}} g(Dsin\alpha, \alpha+\beta) s(rcos(\beta+\alpha-\phi) - Dsin\alpha) Dcos\alpha\, d\alpha\, d\beta \tag{14}$$

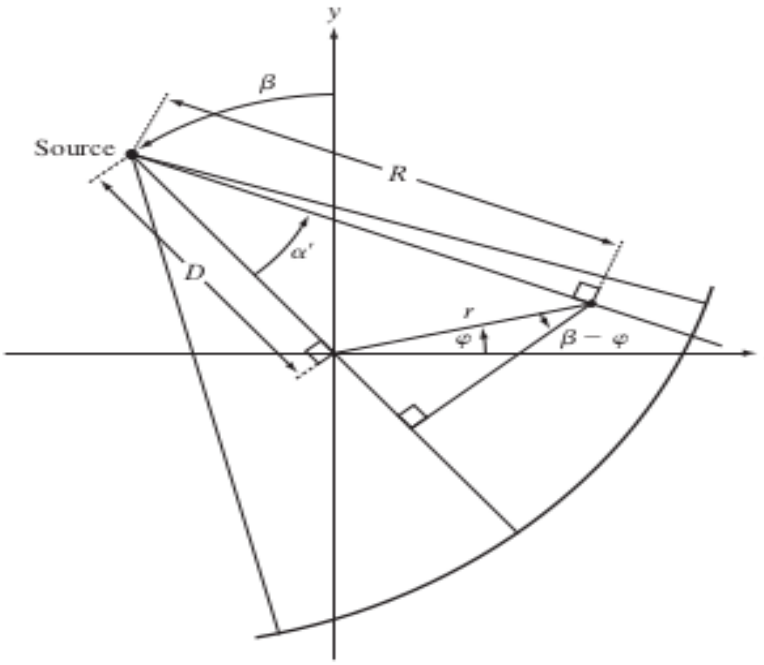

Figure 7: Relationship between angles in fan beam

Rewriting the argument in the following form :

$$rcos(\beta + \alpha - \phi) - Dsin\alpha = rcos(\beta - \phi)cos\alpha - [rsin(\beta - \phi) + D]sin\alpha$$

Let us denote the distance from the x-ray source to the point of reconstruction by R and the detector angel of the ray that passes through (r,ϕ) by α', then we get :

$$Rcos\alpha' = D + rsin(\beta - \phi), \quad Rsin\alpha' = rcos(\beta - \phi) \tag{15}$$

Combining we get :

$$rcos(\beta + \alpha - \phi) - Dsin\alpha = Rsin(\alpha' - \alpha)$$

$$f(r, \phi) = 1/2 \int_0^{2\pi} \int_{-\alpha_m}^{\alpha_m} p(\alpha, \beta) s[Rsin(\alpha' - \alpha)] Dcos\alpha \, d\alpha \, d\beta \tag{16}$$

2.7.3 Filters and Convolution

The problem is basically with the factor $|\omega|$ as it tells us about the amplitude of the frequency we choose in Fourier domain. So as the higher frequencies doesnot have that

much of data in Fourier domain , so due to this noise in higher frequencies the image is much disturbed. The solution to this problem is that we can take this factor $|\omega|$ as filter which is applied to the frequency domain. This filter is generally a Ramp filter whose graph becomes zero outside certain frequency interval where it is defined.

Convolution: Suppose we take two functions f and g on real line. Then if we want to examine the graphs of these functions when it overlapped or shifted sidewards. Then we have to calculate the product of these two functions. These is called convolution defined as :

$$(f \star g)(x) = \int_{-\infty}^{\infty} f(t)g(x-t)\,dt$$

In polar coordinates the equation is :

$$(f \star g)(t,\theta) = \int_{-\infty}^{\infty} f(s,\theta)g(t-s,\theta)\,ds$$

So we need to get a function which is equal to $|\omega|$ which gives fair reconstruction of f. The backprojection equation becomes :

$$\int_0^{\pi} [s(\rho) \star g(\rho,\theta)]_{\rho=xcos\theta+ysin\theta}\,d\theta$$

$$= \int_0^{\pi} [\int_{-\infty}^{\infty} g(\rho,\theta)s(xcos\theta + ysin\theta - \rho)\,d\rho]\,d\theta$$

In simple terms we can say that to reconstruct f we need to do the convolution of the Radon Transform with that function with backprojection. We use a low pass filter called Ramp[6][3] filter to filter the backprojections.

Window Function :

Equation 13 of FBP tells us about from where we can get the original image. The absolute value of $|\ \omega\ |$ integrates to infinity,so we can multiply with a function called window function. Here we use the window function as Hamming window function. The 1D FFT is given by :

[6]Also known as *Ram-Lak filter* named after Ramachandran and Lakshminarayanan[1971]

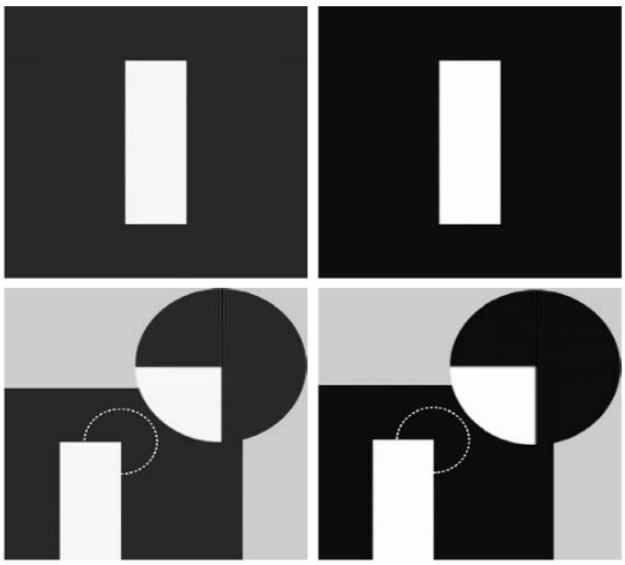

Figure 8: Filtered Backprojection of rectangle using a)Ramp filter and b)Ramp filter with Hamming window

$$h(\omega) = \begin{cases} c + (c-1)cos2\pi\omega/(M-1), & 0 <= \omega <= (M-1) \\ 0, & \text{otherwise} \end{cases} \tag{17}$$

For c = 0.54,the function is called Hamming window[1] and for c=0.5 , it is called Hann Window [2]. Hence multiplication of filter and window function we the get the convolution.

[1]named after Richard Hamming

[2]named after Julius von Hann

3 State of Art

Here we are studying on some of the techniques for reconstructing a human face and seeing which one of these techniques is best. The methods here are different from analytic method and mostly focuses on rendering of the voxels of the image and look on improvements being made on each of those methods.

3.1 3D Reconstruction of Face

As a human face has various regions which includes tissues and hard bones, we survey on various 3D reconstruction approaches and we conclude which is suitable approach for specific range of application.[8]

3.1.1 Introduction

For lower risk surgery and more accuracy we use computer based surgical planning which requires subtle amount of time in preoperatory planning and simulation which helps the doctors to correctly predict the outcome of the surgery. We focus in craniofacial area which includes the bones of skull and face and also the underlying soft tissues and the scalp. Normally the abnormality is cleft lip and palate. Here we take the portion which is suspected to infected by cancer. We take two pictures and any angle and extract 35 features from the two images. Pose estimation is done and we compute the 3d coordinates from the feature points. With interpolation process carried away the texture map are calculated. After this the data of interpolation and texture map is combined to get 3d model .[14] Voxels are manipulated for set of images and the region information is extracted using projection. This 3d model from the slices gives advantages to the doctor in rotation, slicing tilting, RIO extraction. The image is a DICOM[3] image. The techniques are classified as :

[3]Standard in which the image is stored

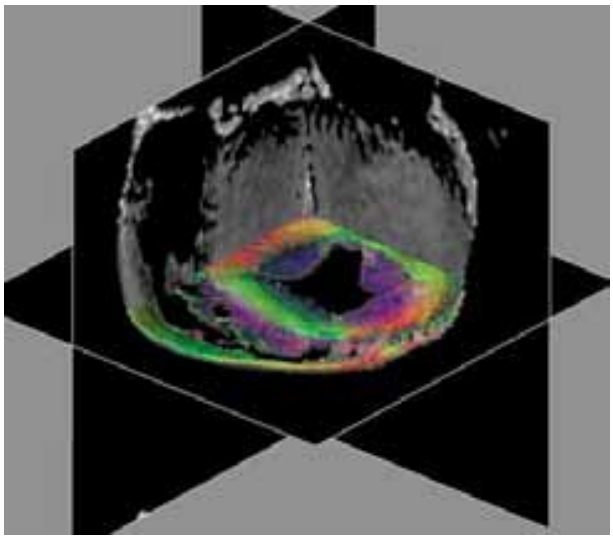

Figure 9: Multiplanar Rendering Illustration

3.1.2 Multiplanar Rendering

Process of converting image acquired from axial to another plane. Slices in axial plane are rendered into coronal and sagittal plane which allows us to view from side or from front to back.[1] MPR studies can be obtained in any plane.
Advantages :

1. One is not restricted to viewing in the direction the data was scanned,which makes it possible to visualize data that was measured in different slices in one 2D image.

2. Its speed also gives it a plus point and also these reformatted data can be used to generate MIP(Maximum/ Minimum Intensity Projection)

Drawback is that the visualized data is 2D as MPR works in 2D. These single image does not give much information in 3D structures than the measured slices. Softwares like OrisWin and Radiant DICOM viewer are used to do this reformatting.

3.1.3 Surface Rendering

Used to visualize the object by means of image data as hard set of certain basic elements like voxels, their faces, other polygons, line segments and points. Also called as indirect

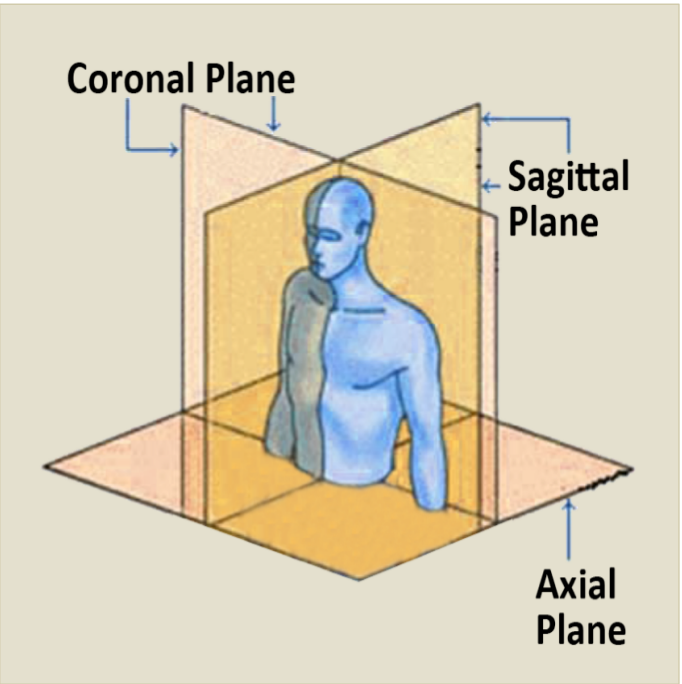

Figure 10: Three Planes(Axial,Coronal,Sagittal)

volume rendering. Two methods of constructing an iso-surface from data volume are :

Contour based surface reconstruction

- Consists of iso-contours which are extracted from each slice can be connected to create iso-surfaces.
- We construct a surface over a set of cross-sectional contours.[9]
- Contours are expected to be non intersecting i.e no contours intersect with itself and other contours within the same slice.
- The images are stored in layers,each containing one or more slices with transparent spacers of appropriate thickness.
- Resulting semitransparent stack roughly approximates the 3D structure.

Marching Cube

This algorithm is well known method for generating a 3D mesh from voxels. Uses a look-up table to determine how a surface intersects a cube and marches to the next

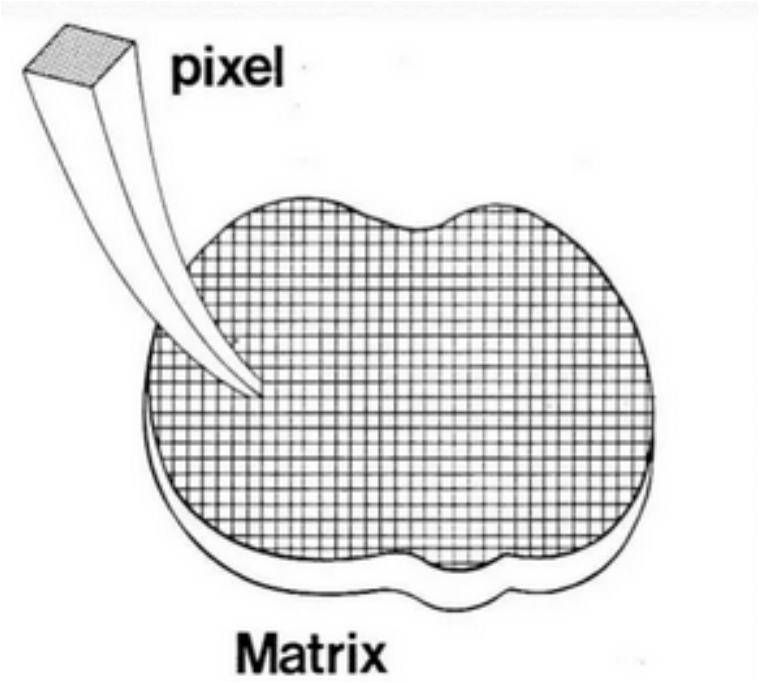

Figure 11: Pixel representation

cube. From four corners in two slices eight vertices are generated. To find the surface intersection , assign one to cube's vertices if their data values exceeds or equal to the value of the surface we are reconstructing and make them inner vertices. Having eight vertices in each cube, there are 256 ways a surface can intersect the cube. Using the reverse and symmetric properties of the cube we can reduce that 256 ways to 15 patterns. This algorithm processes the 3D medical data in scan-line order and calculates triangle vertices using linear interpolation. The process are in three steps -

Segmentation to slices to get the information. Output of segmentation as the input of the algorithm which gives isosurface which we need. Voxels created will be searched. To enhance the efficiency the voxels that intersect with the isosurfaces are only searched. As large amount of triangle mesh is generated we should take measure to merge some of them before rendering and we do this optimization using normal and space constraint. Condition for merging two vertexes are satisfied for two constraints and the triangle mesh is deleted.

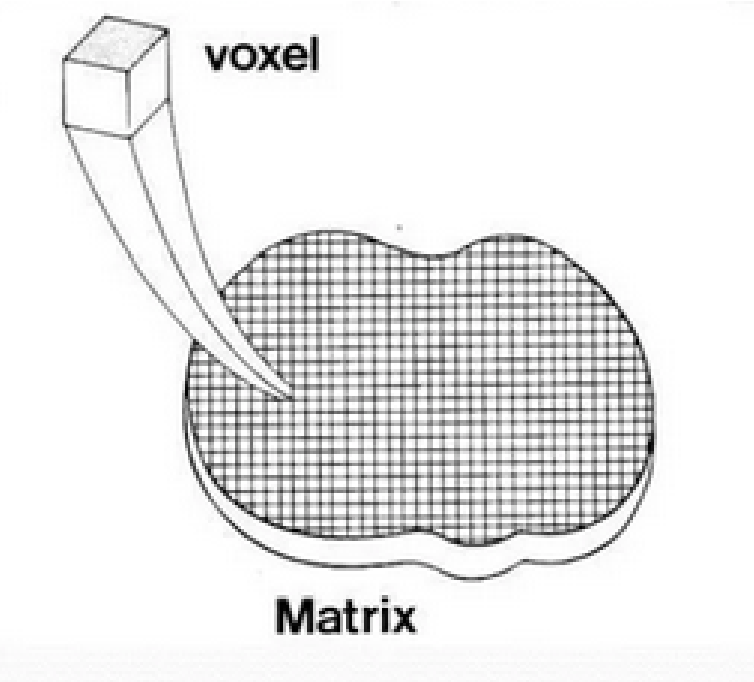

Figure 12: Voxel representation

3.1.4 Volume Rendering

Done using backward mapping method also known as Ray Casting method where a ray is fired from each pixel in the view plane,data from all the voxels intersecting the current pixel is gathered.[11] It's goal is to allow the best use off 3D data and not attempt to impose any geometric structure on it. Surface rendering fails to tell that the data may originate from fluids or other materials which are partially transparent . This problem is solved in volume rendering.

In this process it is to create a 2D image from sampled 3D values. It doesnot use a hard set of basic elements to visualize the image , but implicitly defines the model considering the entire image region to be semi transparent volume. Voxels are not displayed directly in the process, but the values from voxels are used by the transfer function to colorize the data set.[2]

Table 1: Comparative analysis of different 3D reconstruction technique

Method Name	Merits	Demerits	Performance
Multiplanar Rendering[3]	1.It is possible to visualize data that was measured in different slices in a single 2D image. 2.Speed of the method	Visualization is in 2D only	Performance increases when the number of iteration increases.
Contour based surface Rendering[1]	Algorithm is efficient and it reduces the search space	Ambiguities in connecting the contour	Computation cost decreases
Marching Cube Algorithm[2]	Simple to follow the steps	Generation of ambiguous surface and huge quantities of triangular patches.	Computation is fast and results have good resolution
Improved Marching Cube Algorithm[4]	1.Reduces the triangular patches. 2.Increased speed and quality.	More computations are needed	Takes less time than standard MC algorithm to finish the reconstruction without compromising the quality of results
Volume rendering by the Ray Cast alg orithm[8]	Realize real-time rendering with high quality for most medical volume data on visualization	More computations are needed	Avoid rendering delay and the quality of result is very high

Figure 13: Comparative analysis

3.1.5 Results and Notes

Between each pair of contours surfaces can be constructed which can be associated with certain cycles which assists in finding paths and finding such paths reduces the search space. Improved Marching Cube Algorithm reduces the quantity of triangular patches generated and takes less time to finish reconstruction.

Improved Marching Cube Algorithm shows high performance than other techniques and gives best results in reconstruction.

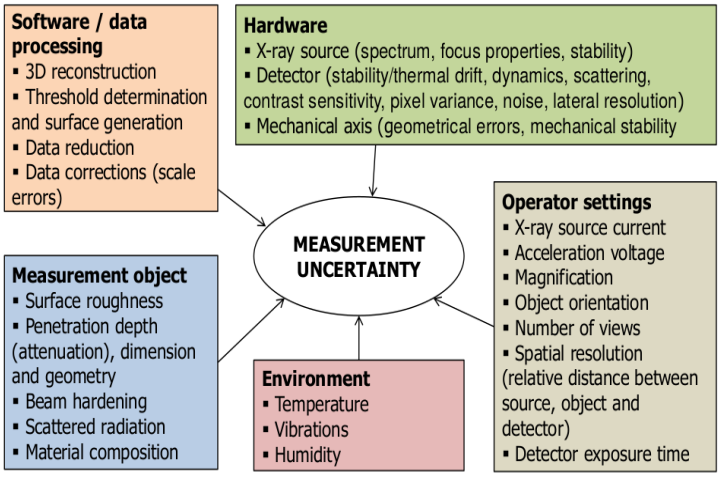

Figure 14: Parameters of CT

4 Discussions

Here we discuss about various parameters where CT reconstruction and how we optimize the resultant out of reconstruction. Also we'll see how we prototype a Cutting Cutting Guide(CCG) which is helpful for pediatric osteotomy.

4.1 Parameters on CT

As we worked on CT reconstruction there are several parameters we got which we have to look about , the parameters are as follows: With great advantages of CT to the medical field, the main problem with CT is increased radiation exposure incurred by the patients.To reduce patient's radiation dose, following are the parameters that a radiologist can change while changing the scan protocols.[13] Let us look these parameters briefly one by one:

4.1.1 Slice Thickness

Slice thickness is normally determined by the width of the collimator.Collimator is used as to reduce exposure of the X-rays and also controls the slice thickness ranging from 1 mm to 3 mm. It also regulate the thickness of the voxel length. Now the question

come how those slice thickness impact the image. If the decrease the thickness,there is increase in image noise as number of photons with each voxel decreases. Maintaining constant noise levels with an image of smaller slice thickness,we should increase radiation dose consequently. So that the slice thickness is not small we also increment the thickness each time. Due to user-specified level of acceptance , the slice thickness and radiation dose depends on each CT scanner and software being used. Larger the slice thickness lesser the radiation dose.

4.1.2 Current

It is the current that is generated by the X-ray tube and it also impacts the image quality how we change the current while scanning the object. Increasing the current greatly enhances the image quality but it also increase the patient's radiation dose.Linear relationship between tube current and patient dose. Nowadays the tube current is controlled by automated tube current modulation rather than manually controlled. These softwares increases the mAs in parts with less attenuation and vice versa. In shoulder and hips increase in mAs and in abdomen and thorax decrease the mAs. If effective mAs or mAs per slice is maintained ie constant, the noise level remains unchanged.

4.1.3 Tube Voltage

Voltage of X-ray tube also plays an important role in reduction of radiation dose. Normally radiation dose changes with reduction of kVp. Since reduction in mAs was linear and had predictable effect to contrast-to-noise ratios,but reduction in potential is non-linear and there is exponential increase in image noise. Low potential are widely accepted and it still preserves image quality. No such tools to correctly select appropriate kVp, so it is totally onto the radiologist to decreasse the kVp looking at the type of study and portion of the body. Algorithms becoming unsatisfactory due to the distribution of fat in patient's body which impacts image quality. Data regarding the correct kvP is still evolving.

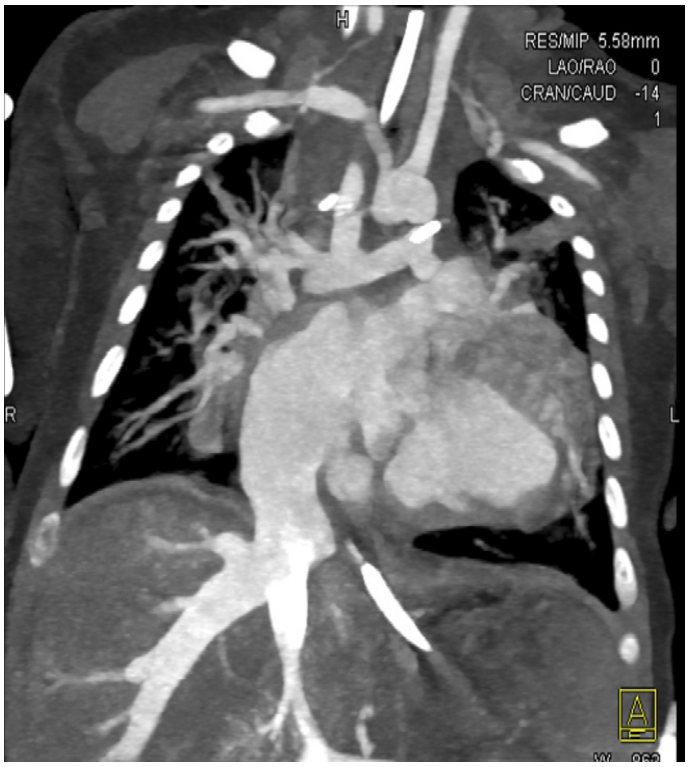

Figure 15: Chest CT at 80 kVp

4.1.4 Patient Orientation

Improper orientation can cause huge impact on image and patient dose.With small variations like 6cm it can result to 22% increase in noise. Specially for patients with smaller body extra attention have to be performed.

Bowtie filters compensate for patient's attenuation. It assumes that the patient is positioned correctly within the gantry. Horizontal positioning isn't a problem but inn vertical axis it becomes tricky.

4.1.5 Radiation Dose

The unit of measurement of the absorption of ionizing energy per unit mass of matter is Milligray. Increase in detector exposure time, scanning time increases but the noise is greatly reduced. **Note :** Contrast materials are given to patients to highlight features in the image when we take CT. It helps the radiologists to diagnose medical conditions.

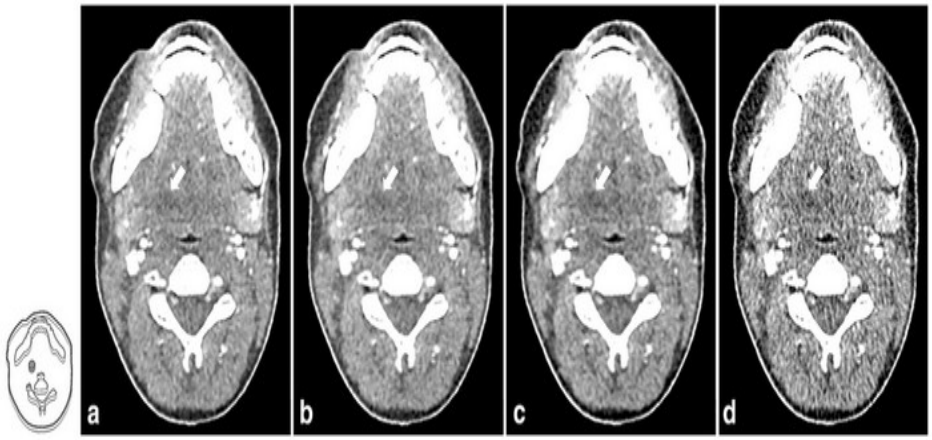

CT images illustrating the effects of tube voltage reduction, tube current reduction, and the image reconstruction method used. a Reference protocol (120 kVp, TCM SD of 7.5, pitch of 0.813, AIDR 3D). b Reduced tube current (120 kVp, TCM SD of 14, pitch of 0.813, AIDR 3D). c Reduced tube voltage and tube current (100 kVp, TCM SD of 14,

Figure 16: Changes with Radiation Dose

Various kinds of contrast materials like iodine based or barium sulfate compounds. Can be taken orally, rectally or intravenously i.e through veins using injection.

4.2 CCG Prototyping

In paper [6] we are constructing a CCG which is free from outside intervention and performed osteotomy to pediatric patients. We look upon how a deformity is seen based on HEA and causes severe coxa vara. For prototyping CCG, we looked upon deformmity and based on that we used process of FDM to create a prototype of guide the surgeons in surgery. Basiclly we 3D printed the necessary models with precise calculations and made a 3D printed model of CCG[10]. Simple workflow was adopted to get CCG using various softwares like Meshlab[3], InVesalius etc.

[3]Meshing and Cleaning is done

4.3 Reconstruction and Optimization

In paper [7] CT reconstruction of specific human knee was done and the data was taken from one set of CT images and two sequences of MRI. The data was segmented and model registration was done based on image we got. For each part or soft tissues of the knee different registration was done. After registration a 3D anatomical model of human knee was created. After the reconstruction the model was optimized to remove any problems based on the meshes. Thus with relevant parameters the quality was improved.

5 Conclusion

In this paper we have studied how parallel beam projection method which is based upon Radon Transform when performed lead us to show the relationship between Radon Transform and Fourier Slice Theorem of FFT. Also we have studied on how we reconstruct the image and how it gets affected based on choice of window function. The developed inverse Radon Transform was used to configure the image reconstruction process using window function. We conclude that the mathematical model forms the backbone of the 3D reconstruction technique and looked on various other methods other than analytic methods which was very much useful. Thus we say that in analytic reconstruction the window plays an important role as this window can be used as trade-off between the blur and noise of an image.

References

[1] https://www.science.gov/topicpages/m/multiplanar+reformatted+images.html, 2002. [Online accessed 27-September-2022].

[2] https://en.wikipedia.org/wiki/Volume-rendering, 2011. [Online accessed 28-September-2022].

[3] https://pylops.readthedocs.io/en/latest/tutorials/ctscan.html, 2012. [Online accessed 22-August-2022].

[4] https://en.wikipedia.org/wiki/Shepp%E2%80%93Logan_phantom, 2015. [Online accessed 2-August-2022].

[5] T. G. Feeman. *The Mathematics of Medical Imaging*. Springer, 2nd edition, 2010.

[6] L. Frizziero, G. M. Santi, C. Leon-Cardenas, G. Donnici, A. Liverani, P. Papaleo, F. Napolitano, C. Pagliari, G. L. Di Gennaro, S. Stallone, et al. In-house, fast fdm prototyping of a custom cutting guide for a lower-risk pediatric femoral osteotomy. *Bioengineering*, 8(6):71, 2021.

[7] J. B. Junlong Niua, Xiansheng Qina and H. Lib. Reconstruction and optimization of the 3d geometric anatomy structure model for subject-specific human knee joint based on ct and mri images. 2021.

[8] T. S. Kumar and A. Vijai. 3d reconstruction of face from 2d ct scan images. *Procedia Engineering*, 30:970–977, 2012.

[9] D. Mackay. Robust contour based surface reconstruction algorithms for applications in medical imaging. 2019.

[10] H. H. Malik, A. R. Darwood, S. Shaunak, P. Kulatilake, A. Abdulrahman, O. Mulki, and A. Baskaradas. Three-dimensional printing in surgery: a review of current surgical applications. *journal of surgical research*, 199(2):512–522, 2015.

[11] S. Mazziotti, A. Blandino, M. Gaeta, A. Bottari, C. Sofia, T. D'Angelo, and G. Ascenti. Postprocessing in maxillofacial multidetector computed tomography. *Canadian Association of Radiologists Journal*, 66(3):212–222, 2015.

[12] R. E. W. Rafael C.Gonzalez. *Digital Image Processing*. Pearson, 3rd edition, 2008.

[13] S. P. Raman, M. Mahesh, R. V. Blasko, and E. K. Fishman. Ct scan parameters and radiation dose: practical advice for radiologists. *Journal of the American College of Radiology*, 10(11):840–846, 2013.

[14] L. Yu and S. Leng. Image reconstruction techniques. *American College of Radiology*, 2010.